CDF Note 8709

Measurement of the top quark mass in the all hadronic channel using an in-situ calibration of the dijet invariant mass with $943pb^{-1}$

The CDF Collaboration
URL http://www-cdf.fnal.gov
February 22, 2007

Abstract

We present a preliminary measurement of the top quark mass in the all-hadronic channel, using $p\overline{p}$ collisions at $\sqrt{s} = 1.96TeV$ collected at the Collider Detector at Fermilab. Assuming standard model $t\bar{t}$ production and using the matrix element as a weight, an event probability is calculated. The top quark mass is reconstructed for each event by maximizing the event probability, and so Monte Carlo templates are produced, dependent of the true top quark mass and the jet energy scale. The most likely top mass is extracted by fitting the data to the templates distributions. From 72 events observed with $943pb^{-1}$ we measure a top quark mass of $171.1 \pm 3.7(stat. + JES) \pm 2.1(syst.)GeV/c^2$.

Preliminary Results for Winter 2007 Conferences

1 Introduction

The Standard Model is the most successful theory in particle physics. Top quark is one of the fundamental building blocks in this model, but it is the newest in terms of discovery. The properties of this particle such as mass, decay width, charge, production cross-section are known experimentally to a relatively small precision. Improving this knowledge has wide implications in particle physics starting with testing the Standard Model predictions on the top quark and ending with setting limits on the Higgs boson properties, another fundamental piece in the model that is yet to be observed experimentally.

We present a preliminary measurement of the top quark mass in the all-hadronic channel, using $p\overline{p}$ collisions at $\sqrt{s} = 1.96TeV$ collected at the Collider Detector at Fermilab. The CDF detector is described in detail in [2].

At the Tevatron, the pair production is the most dominant channel in producing the top quark and once produced being so heavy it decays before it can hadronize into a W boson and a b quark. The W boson will decay either into two other light quarks or into two leptons. The final state of interest for this analysis is the all hadronic channel, occuring 44% of the time.

Our technique starts by modelling the data using a mixture of Monte Carlo signal and Monte Carlo background events. The events will be represented by two variables: dijet invariant mass and an event-by-event reconstructed top mass. The latter is obtained using a matrix element technique which will be described in section 2. For signal, the shapes obtained in these two variables are parameterized as a function of top quark pole mass and JES. For background no such parameterization is needed. Hence our model will depend on the top mass and the JES. Then we'll interpret the values of top mass and JES that provide the best fit to the data, as the real values.

2 Data Sample & Event Selection

The data events are the Run2 CDF multijet events selected with the $TOP_MULTIJET$ trigger, and it amounts to approximately $943pb^{-1}$.

The final state of the ttbar all hadronic channel will be observed in the detector as 6 jets. However, the same 6 jet signature is produced via other sources, constituting the background events (mostly QCD multijets). In fact the background events are produced in much larger amounts than the ttbar events, and therefore we need to separate the two samples as best as possible. The following set of cuts are designed to enhance the ttbar content of the multijet dataset:

- ask for exactly 6 jets with $E_T > 15GeV$ and $|\eta| < 2$
- Aplanarity $+0.005 * \sum E_{T3} > 0.96$
- Centrality > 0.78
- $\sum E_T > 280GeV$
- ≥ 1 b-tags (identifying secondary vertices)
- $minLKL < 10$

where ΣE_T is sum of all the transverse energies of all the six tight jets in the event, $\Sigma_3 E_T$ is the sum of all the six tight jets minus the two most energetic ones, $Centrality$ is defined in equation 5 and

the *Aplanarity* is defined as 3/2 of the smallest eigenvalue of the sphericity matrix $\hat{S^{ij}}$. The sphericity matrix $\hat{S^{ij}}$ is defined in equation 6.

$$Centrality = \frac{\sum_{j=1}^{6}(E_T)_j}{\sqrt{(\sum_{j=1}^{6}(E_T)_j)^2 - (\sum_{j=1}^{6}(P_z)_j)^2}} \tag{1}$$

$$S^{ij} = \frac{\sum_{p=1}^{6}(P_p^i \times P_p^j)}{\sum_{p=1}^{6}(P_p^2)}, \quad where \quad i,j = x,y,z \tag{2}$$

The last cut provides the most drastic background reduction and it is essentially asking for the event to have a high probability of being a ttbar event. This probability uses the ttbar matrix element to weigh the observed jet configuration. We calculate the a priori probability density for an event to be the result of the $t\bar{t}$ Standard Model production and decay at a given pole mass M_{top}. This probability density has the following expression:

$$P(j|M_{top}) = \frac{1}{\sigma(M_{top})\epsilon(M_{top})N_{combi}} \sum_{combi} \int dz_a dz_b f(z_a) f(z_b) d\sigma(M_{top}, p) TF(j|p) P_T(p) \ . \tag{3}$$

Briefly, it is a normalized integral over the product of the elementary cross-sections, $d\sigma(M_{top}, p)$, of all the possible parton configurations, with the parton distribution functions of the proton and anti-proton, $f_{a,b}$. In the equation 1, j and p are compact notations for the four-momenta of the six jets and of the six partons respectively. In reality, the final state partons are observed as jets in the detector, and their energy can be mis-measured. To account for this, the elementary cross sections are modulated by a weight, called $TransferFunction$ $TF(j|p)$, that relates jets momenta, j, to parton momenta, p. An additional weight, $P_T(p)$, is factored in, representing the transverse momentum spectrum of a $t\bar{t}$ event.The elementary cross-section has the following expression:

$$d\sigma(M_{top}, p) = \frac{|\mathcal{M}(M_{top}, p)|^2}{4E_a E_b |v_a - v_b|}(2\pi)^4 \delta^4(p_a + p_b - \sum_{i=1}^{6} p_i) \prod_{i=1}^{6} \frac{d^3 p_i}{(2\pi)^3 2E_i} \tag{4}$$

In Eq.2, $\mathcal{M}(M_{top}, p)$ represents the matrix element and, barring the numerical factors, it has the following formula:

$$\begin{aligned} \mathcal{M}(M_{top}, p) \approx & \frac{\overline{v}(p_{\overline{q}})\gamma^\mu u(p_q)}{(p_q + p_{\overline{q}})^2} \cdot \frac{\overline{u}(p_u)\gamma^\alpha(1-\gamma^5)v(p_{\overline{d}})}{P_{W^+}^2 - m_W^2 + im_W\Gamma_W} \cdot \frac{\overline{u}(p_d)\gamma^\sigma(1-\gamma^5)v(p_{\overline{u}})}{P_{W^-}^2 - m_W^2 + im_W\Gamma_W} \cdot \\ & \overline{u}(p_b)\gamma_\alpha(1-\gamma^5)\frac{\not{p}_t + m_t}{p_t^2 - m_t^2 + im_t\Gamma_t}\gamma_\mu \frac{\not{p}_{\overline{t}} + m_t}{p_{\overline{t}}^2 - m_t^2 + im_t\Gamma_t}\gamma_\sigma(1-\gamma^5)v(p_{\overline{b}}) \end{aligned} \tag{5}$$

3 Top Mass Templates

We use the matrix element to build the top mass templates. The same event probability mentioned for the event selection is used again, more exactly, its dependence on the top mass is used. This probability will have a minimum in negative logarithmic scale for a certain value of top mass, and this value we'll use to form the top templates. The shape of these templates depends on the input top mass and JES for ttbar events, and they are shown in figure 1.

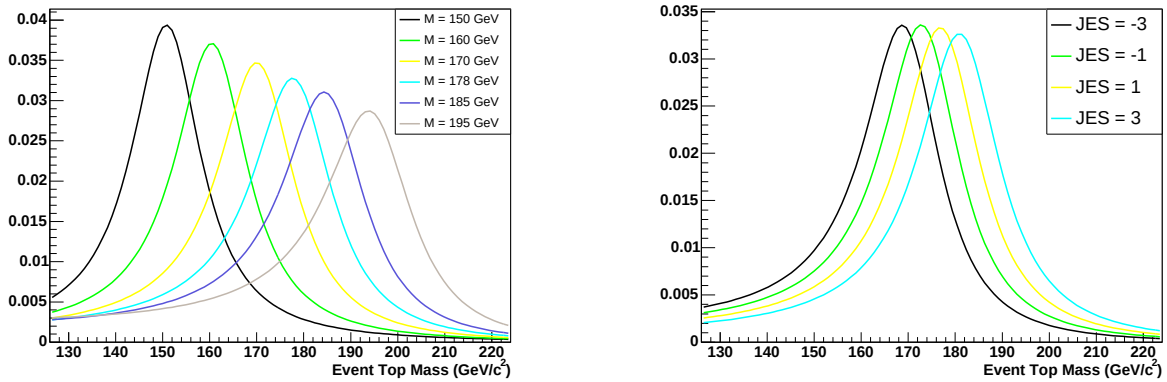

Figure 1: Top templates for ttbar events. The left plot shows the top mass dependence, and the right plot shows the JES dependence.

4 Dijet Mass Templates

The dijet mass templates are formed by considering the invariant mass of all possible pairs of untagged jets in the sample. Their shapes are build for a variety of top mass samples each having several possible JES values. The invariant mass of an untagged pair of jets shouldn't depend on the top mass, but should be sensitive to change in the jet energy scale. The shapes for various ttbar samples are shown in figure 2.

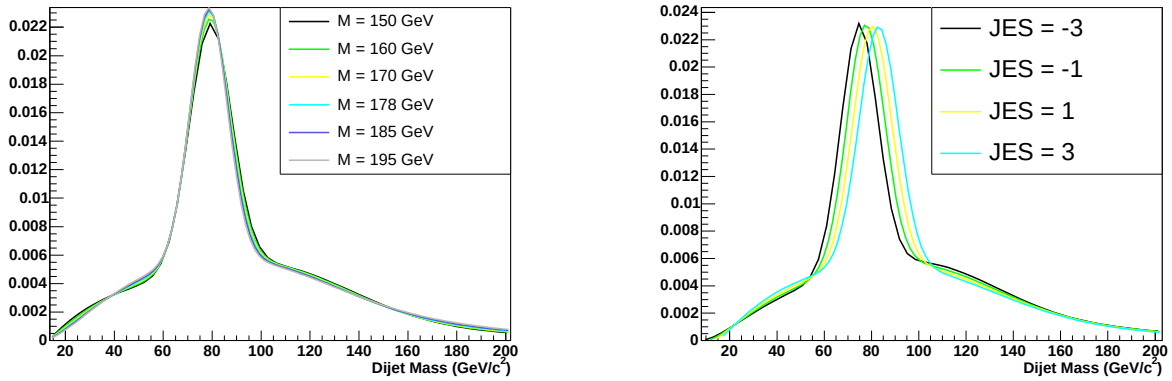

Figure 2: Dijet masss templates for ttbar events. The left plot shows the top mass dependence, and the right plot shows the JES dependence.

5 Background

We use a data-driven background model by extrapolating the heavy flavor rates from background dominated sample into our signal region. This is also known as "Method 1" background model, and it is using the tag rates as determined in the ttbar cross-section analysis described here. The background templates are independent of the top mass or JES. The event top mass templates are shown in figure 3 and the dijet mass templates are shown in figure 4.

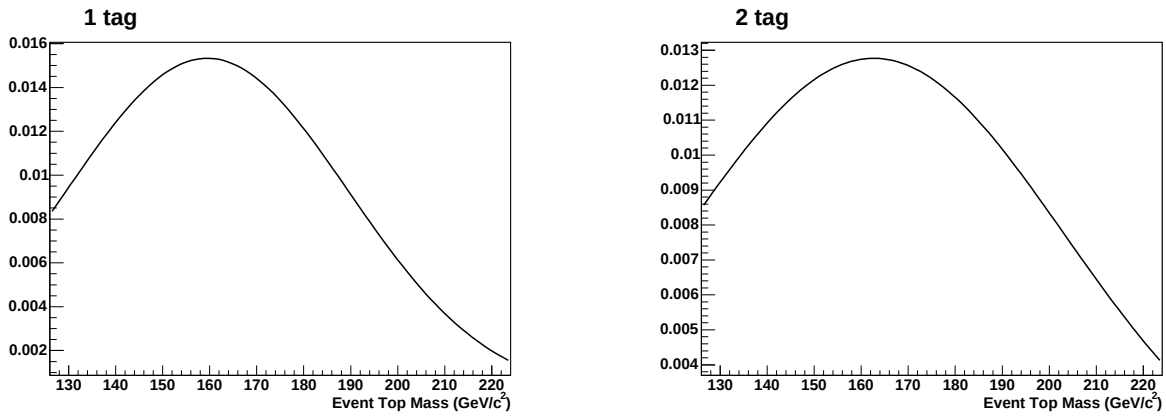

Figure 3: Top templates for background events. The left plot shows the case of single tagged events, and the right plot shows the case of double tagged events.

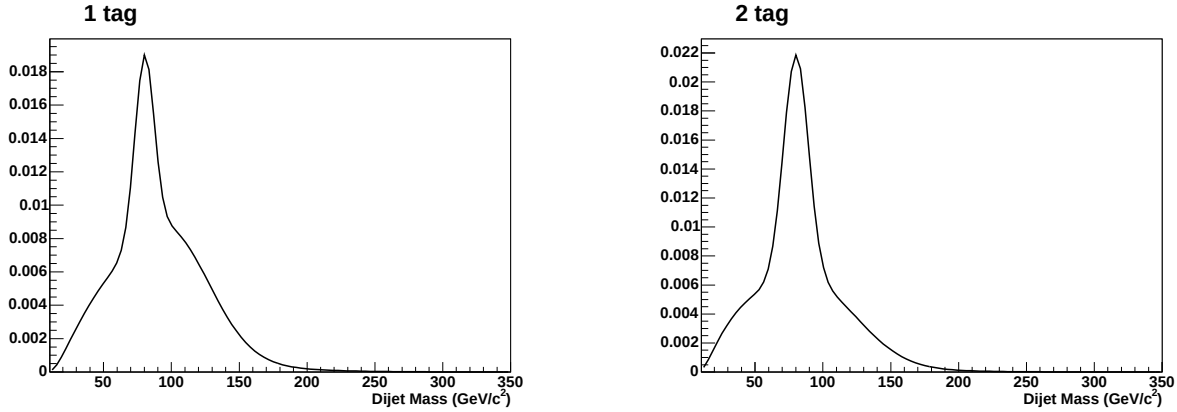

Figure 4: Dijet mass templates for background events. The left plot shows the case of single tagged events, and the right plot shows the case of double tagged events.

6 Validation of the method

We need to make sure that our estimator of the top mass and JES is unbiased and that the sensitivity of the method is well understood. Figure 5 shows the reconstructed values of JES and top mass represented by the red dots versus the true values represented by the dashed lines. The reconstructed values agree within the uncertainties with the true values.

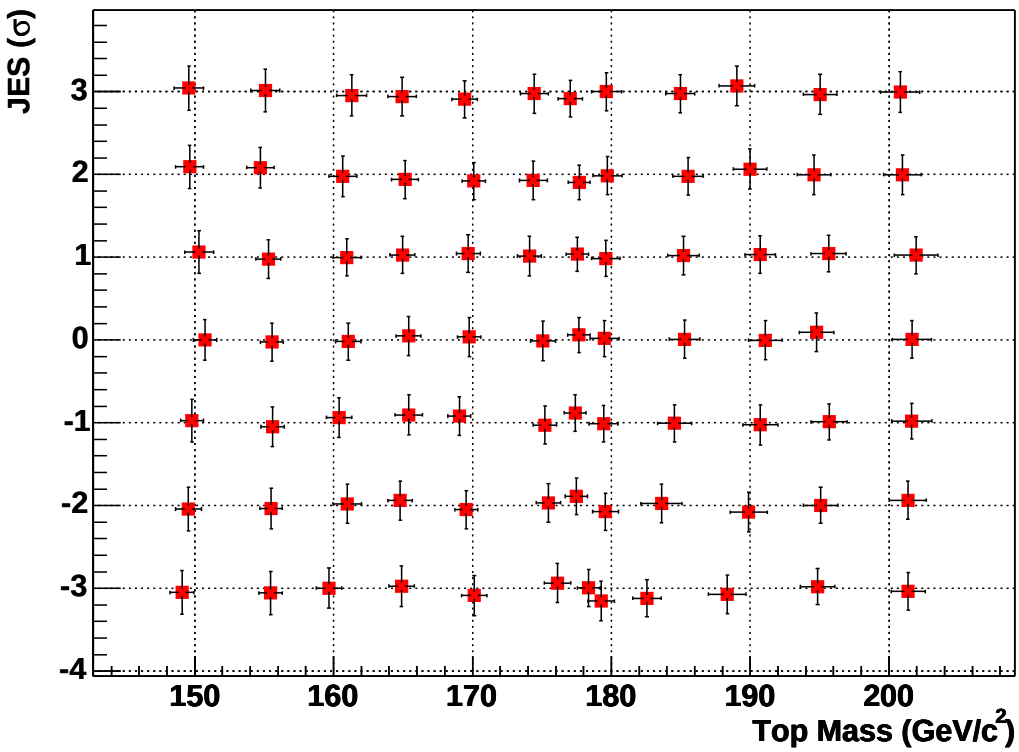

Figure 5: Reconstructed JES and top mass values (red dots) versus the true values (dashed lines). The reconstructed values agree with the true values within the error bars.

The mass pulls mean as a function of JES, shown in left plot of figure 6, confirms our estimator of top mass as being unbiased. However, the mass pulls width as a function of the JES is on average 1.13, which means we need to inflate the uncertainty on the top mass by 13%.

7 Systematic Uncertainties

The largest sources of systematic uncertainty are summarized in table 1. The jet energy scale is treated as a nuisance parameter in this analysis, and is constrained both by the a priori calorimeter calibration and the statistical information from the W mass through the dijet mass of the event. It is

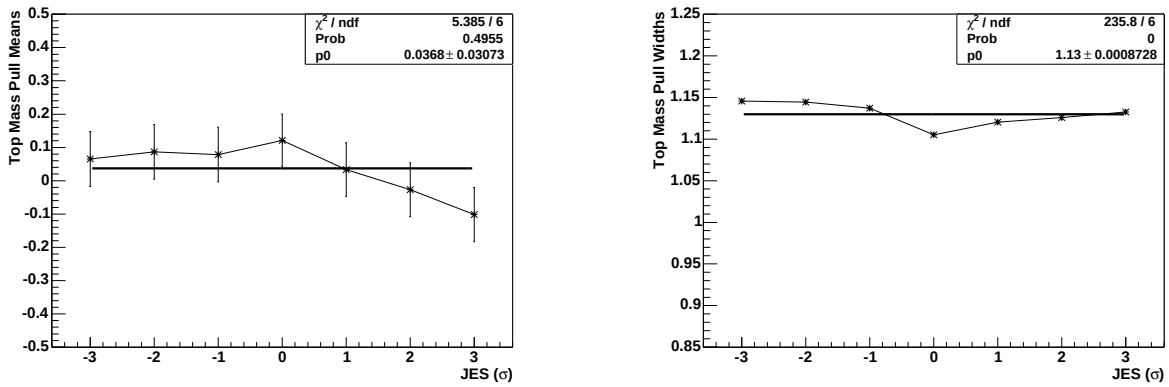

Figure 6: The left plot shows the mass pulls mean versus JES, and the right plot shows the mass pulls width versus JES.

included in the uncertainty arising from the likelihood fit, thus not considered a traditional source of systematic uncertainty.

Source	Value (GeV/c^2)
ISR	0.3
FSR	1.2
PDF	0.5
Generator	1.0
Method Calibration	0.2
Background Shape	0.9
Background Statistics	0.4
Sample Composition	0.1
b-JES	0.4
Residual JES	0.7
Total	2.1

Table 1: Table of systematics uncertainties.

8 Results

We have applied the method described in the previous section to the data events corresponding to $943pb^{-1}$. In table 2 we show the input values as well as the reconstructed ones for the number of events in the sample. The number of signal events corresponds to a theoretical cross-section of $6.7pb^{-1}$ as determined in [1]. The uncertainties on the number of signal events follows a Poisson and it's larger than the systematic uncertainty due to the theoretical cross-section.

Parameters	Input	Output
Total (1tag)	48	47.8
Signal (1tag)	13(3.6)	13.2(3.7)
Background (1tag)	35	34.6(7.2)
Total (2tags)	24	23.3
Signal (2tags)	14(3.7)	14.1(3.4)
Bakground (2tags)	10	9.2(4.3)

Table 2: Number of events for the $t\bar{t}$ expectation and for the observed total for a luminosity of $L = 943pb^{-1}$ passing all the cuts. The input values for signal have the uncertainties next to them in paranthesis. The background expectation being the difference between total and signal is also shown. For the output values, the numbers in the paranthesis are the uncertainties.

The measured top mass is $M_{top} = 171.1 \pm 3.7 GeV$, while the measured JES is $JES = 0.5 \pm 0.9$. The quoted uncertainty on the top mass contains both the statistical component and the JES contribution.

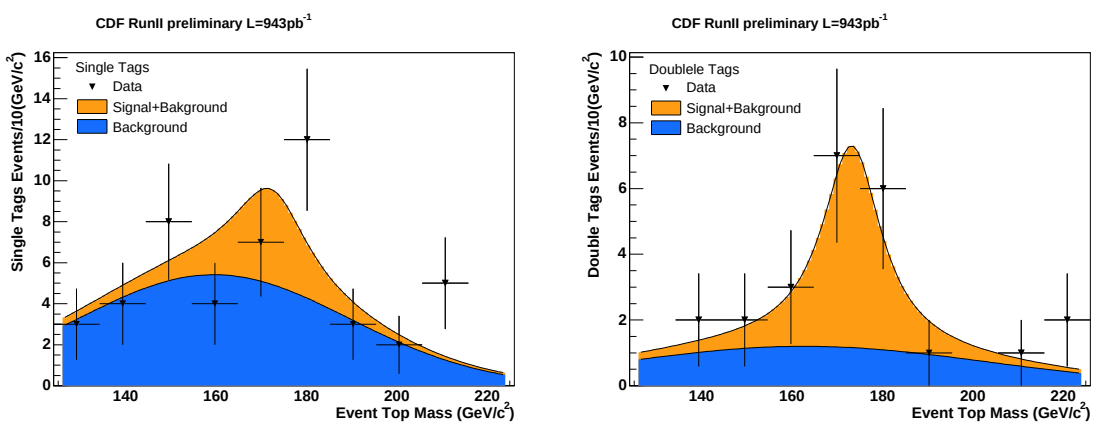

Figure 7: The event reconstruted top mass for data (black points), signal+background (orange) and only background events (blue). Single tagged sample is on the left, while the double tagged sample is on the right.

We thank the Fermilab staff and the technical staffs of the participating institutions for their vital contributions. This work was supported by the U.S. Department of Energy and National Science Foundation; the Italian Istituto Nazionale di Fisica Nucleare; the Ministry of Education, Culture, Sports, Science and Technology of Japan; the Natural Sciences and Engineering Research Council of Canada; the National Science Council of the Republic of China; the Swiss National Science Foundation; the A.P. Sloan Foundation; the Bundesministerium fuer Bildung und Forschung, Germany; the Korean Science and Engineering Foundation and the Korean Research Foundation; the Particle Physics and Astronomy Research Council and the Royal Society, UK; the Russian Foundation for Basic Research; the Comision Interministerial de Ciencia y Tecnologia, Spain; and in part by the European Community's Human Potential Programme under contract HPRN-CT-20002, Probe for New

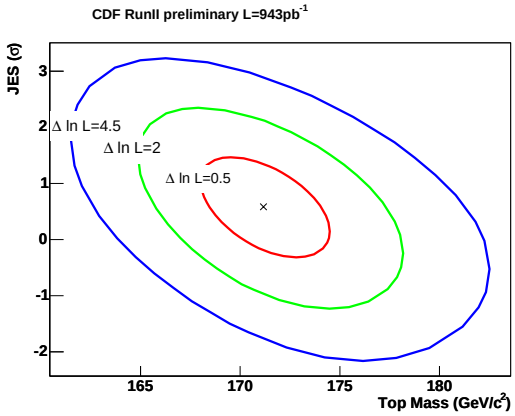

Figure 8: The 1-sigma (red), the 2-sigma (green) and the 3-sigma (blue) contours of the mass and JES reconstruction in the data.

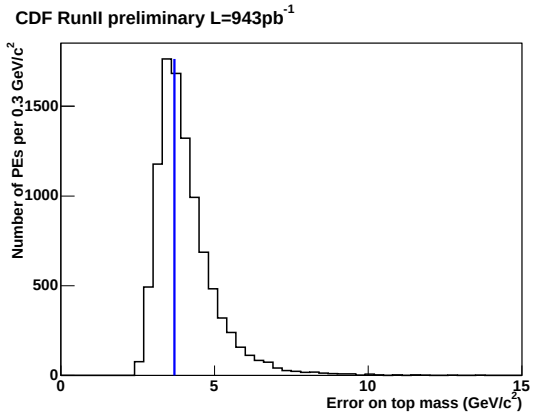

Figure 9: Histogram shows the expected statistical uncertainty from Monte Carlo using pseudo-experiments, while the line shows the measured one. About 41% of all pseudo-experiments have a lower uncertainty.

Physics.

References

[1] M. Cacciari, et al., The $t\bar{t}$ Cross-section at 1.8 TeV and 1.96 TeV: A Study of the Systematics due to Parton Densities and Scale Dependence, JHEP **404**, 68 (2004).

[2] F. Abe, et al., Nucl. Instrum. Methods Phys. Res. A **271**, 387 (1988); D. Amidei, et al., Nucl. Instum. Methods Phys. Res. A **350**, 73 (1994); F. Abe, et al., Phys. Rev. D **52**, 4784 (1995); P. Azzi, et al., Nucl. Instrum. Methods Phys. Res. A **360**, 137 (1995); The CDFII Detector Technical Design Report, Fermilab-Pub-96/390-E

[3] T. Sjostrand et al., High-Energy-Physics Event Generation with PYTHIA 6.1, Comput. Phys. Commun. **135**, 238 (2001).

[4] G. Corcella et al., HERWIG 6: An Event Generator for Hadron Emission Reactions with Interfering Gluons (including supersymmetric processes), JHEP **01**, 10 (2001).